

Methane Fluxes at the Water–Atmosphere Interface in the Southern Tatar Strait of the Sea of Japan: Distribution and Variation

R.B. Shakirov✉, M.G. Valitov, N.S. Syrbu, A.V. Yatsuk, A.I. Obzhirov, V.F. Mishukov, E.V. Lifanskii, O.V. Mishukova, A.S. Salomatin

*V.I. Il'ichev Pacific Oceanological Institute, Far Eastern Branch of the Russian Academy of Sciences,
ul. Baltiiskaya 43, Vladivostok, 690041, Russia*

Received 7 February 2018; received in revised form 17 November 2019; accepted 27 November 2019

Abstract—We present the results of gas-geochemical surveys in the sea surface water layer, water column, and bottom sediments of the Tatar Strait (north of the Sea of Japan) in 2012, 2014, 2015, 2017, and 2018. The distribution of methane fluxes at the water–atmosphere interface is examined, and its relationship with the geologic structure of the Tatar Strait area is discussed. Methane emission has been revealed throughout most of the Tatar Strait area. The most intense methane fluxes at the water–atmosphere interface, up to 482 mol/(km²×day), are observed on the gas-bearing southwestern shelf and on the gas hydrate slope of Sakhalin Island. The high concentrations of methane in seawater and the high contents of methane, hydrogen, and helium in the shelf and slope bottom sediments are probably due to the seismotectonic activity in the region, the presence of gas hydrates, gas concentration zones, gas migration channels, and the regional deep structure. Application of the model for calculation of the flux and impurity transfer fields to the studied water area has shown high methane emission from the sea surface in areas of vertical gas migration from lithospheric sources. The contribution of hydrodynamic factors to the formation of such zones of high methane emission is less than that of geologic factors. The obtained data on methane flux at the water–atmosphere interface for a shallow sea gave a detailed insight into the main gas discharge zones in the southern Tatar Strait.

Keywords: methane distribution; methane fluxes; Sea of Japan; Tatar Strait

INTRODUCTION

Gas-geochemical studies provide information about the composition, genesis, and mechanisms of spread of natural gases and the quantitative parameters of their migration at the lithosphere–hydrosphere and hydrosphere–atmosphere interfaces of marginal seas. The latter issue is particularly important for taking account of the role of marginal seas in the balance of the atmospheric greenhouse gases. The processes of gas supply from various lithospheric sources are comprehensively studied both in the western and in the eastern Pacific. Methane releases along with gases seeping out of hydrocarbon accumulations. These gases serve as indicators of hydrocarbon deposits and mark zones of atmospheric methane emission. Mau et al. (2007b) studied natural-gas seepage out of coastal coal and oil fields in the Pacific near Santa Barbara, California. The amounts of seeping methane were determined at 79 stations in an area of 280 km², with the largest ones recorded in an area of no less than 70 km². Such studies are also actively performed in the Arctic, a region with specific gas generation and gas transfer. In the western Arctic Ocean, the desalinated surface water layer

limited atmospheric methane emission (Fenwick et al., 2017). Mau et al. (2017) examined a large area along the western Svalbard margin (from 74 to 79 °N), where thousands of gas seeps were recorded, and showed that the dissolved methane plume is hundreds of kilometers long. Such methane plumes were also recorded in the marginal water areas of the Pacific (Suess et al., 2001; Mau et al., 2012). In the water column, methane plumes or anomalous methane fields are observed as disc-like areas at different depths on the eastern shelf and on the slope of Sakhalin in the Sea of Okhotsk (Mishukova et al., 2007, 2010). Recently, they have also been revealed in the water area of the Tatar Strait in the Sea of Japan (Mishukova et al., 2015). Nevertheless, the mechanisms of gas discharge from geologic structures into the water column and then into the atmosphere have been poorly studied. Kvenvolden and Rogers (2005) studied the catastrophic methane exhalations resulted from the decomposition of CH₄ hydrate and the macro- and microseepage of CH₄ out of mud and magmatic volcanoes and in geothermal areas and ocean fault zones. They assumed that these exhalations affected global climate changes in the past. Seismic activity is one of the crucial factors controlling methane emission; it can both intensify and weaken gas fluxes. For example, study of methane release on the Costa Rica coast revealed its inverse relationship with seismotectonics: Obviously, the earthquakes that took place in 2002

✉ Corresponding author.

E-mail address: ren@poi.dvo.ru (R.B. Shakirov)

closed methane migration paths and thus reduced methane emissions (Mau et al., 2007a). Until recently, it has been believed that submarine gas seepage caused by earthquakes are the natural way of carbon release from sedimentary strata into the hydrosphere and do not significantly contribute to the budget of the local or global carbon cycle. At present, the effect of earthquakes on abnormal methane emission has been established in different regions of the World Ocean. Fischer et al. (2013) believe that the seismic activity in the Arabian Sea, especially after the $M = 8.1$ earthquake in 1945, disturbed the gas hydrate-bearing strata, which favored the intense free migration of gas and thus led to a great number of methane seeps. The most favorable conditions for this scenario are in the Sakhalin water area of the Sea of Okhotsk and the Sea of Japan (Shakirov et al., 2016).

Water-dissolved methane, hydrogen, and helium are used as indicators of fault zones and for the prediction of seismic activity, the environmental assessment, and the search for hydrocarbon fields (Obzhairov, 1993; Shakirov et al., 2016). These gases are also important gas-geochemical indicators of caustobioliths, such as gas hydrates (Shakirov et al., 2016). Joint anomalies of methane and helium may indicate an ascending mantle fluid. Gasometric research permits mapping permeable faults. Study of the distribution of helium, gas hydrocarbons, and hydrogen and of their isotope characteristics is of special interest: The correlation between these parameters and the geologic structure of the area permits one to identify long-living gas sources and permeable zones of different activities.

In general, approaches to the assessment of methane emission at the water–atmosphere interface must be further developed, because the remote-sensing methods are still not precise and *in situ* experimental studies are not systematic. In the course of study of the emission of methane, one of the most active contributors to the greenhouse effect, it is extremely important to apply an integrated approach taking into account geologic, hydrologic, and meteorologic factors. This approach helps to implement an integrated geological, geophysical, and oceanographic areal field research.

The goal of this work is to discuss new data on the distribution of methane fluxes at the water–atmosphere interface in the Tatar Strait and to analyze the influence of geologic and hydrometeorologic factors on the methane content in water and bottom sediments.

BRIEF OUTLINES OF THE STUDY AREA

The study area covers the South Tatar sedimentary basin localized in a depression in the south of the Tatar Strait.

Figure 1 shows a schematic tectonic map of the basin, simplified and supplemented after Zharov et al. (2004) and Kharakhinov (2010).

The South Tatar depression is bounded by the East Primorye fault zone in the west and the West Sakhalin fault zone in the east. The latter zone includes volcanoes that

were active 5–10 Myr ago (Mel'nikov and Il'ev, 1989). In general, the Tatar Strait is a large rift trough 1200 km in length and 60–300 km in width. The western continental coast is composed mostly of weakly dislocated Cenozoic or, seldom, Upper Cretaceous volcanics of intermediate and mafic composition. In the West Sakhalin depression extending along the Sakhalin coast of the Tatar Strait, there are local exposures of dislocated Upper Cretaceous, Paleogene, and Neogene terrigenous and volcanic deposits. The same deposits, including coal-bearing ones, are traced westward at the base of the strait. The rift nature of the depression is responsible for a high heat flux (67 to 171 mW/m²) and gas fluid permeability channels in the sedimentary strata (Kharakhinov, 2010; Rodnikov et al., 2014).

The earlier study of gas-geochemical fields in the bottom water of the Tatar Strait yielded a number of important results (Obzhairov, 1993) indicating anomalous methane fields (with CH₄ concentrations of up to 45 nmol/L) and the petroleum potential of the sedimentary strata. Later, studies within the International Sakhalin Slope Gas Hydrate Project (Jin et al., 2013) revealed that the upper part of the sedimentary section, especially that in the eastern part of the South Tatar depression, has numerous chimneys, which usually mark gas flares and gas hydrates in the upper bed of sedimentary strata. Studies of the distribution of gas hydrocarbons, the carbon isotope composition of methane and ethane, and the concentrations of hydrogen and helium in the chimney zone showed a predominance of catagenetic gases in the gas hydrate clusters (Shakirov et al., 2016). Gas hydrate-bearing structures were mapped mainly in the area of the Sakhalin slope (Minami, 2016), i.e., on the eastern flank of the South Tatar depression.

These and other specific features of the South Tatar sedimentary basin indicate that it must actively supply methane from bottom sediments not only to water but also to the atmosphere.

MATERIALS AND METHODS

The research was performed in the southern part of the Tatar Strait of the Sea of Japan. The schematic map of the study area is shown in Fig. 2. Materials for the study were sampled during the expeditions of the R/V Akademik M.A. Lavrentiev (cruise LV-59, August 2012; cruise LV-62, June 2013; cruise LV-67, June 2014; and cruise LV-70, June 2015) and the R/V Akademik Oparin (cruise OP-54, September–October 2017 and cruise OP-55, October 2018).

The main research was carried out in the southern part of the Tatar Strait, where surface water, water from the water column, and cores of the bottom sediments were sampled in 2012–2018. In the northern part of the Tatar Strait, where the North Tatar sedimentary basin is located, only surface water was sampled in the autumn of 2017 and 2018 (R/V Akademik Oparin, cruises OP-54 and OP-55). Three cruises were organized in the early summer (June); one, in August;

and two, in the autumn. These expeditions helped to make a regular observation network within the study area (Fig. 2), which is an important condition for the interpretation of methane fluxes.

Water sampling and analysis technique. Seawater for analysis for CH₄ was sampled at a depth of 4 m from the sea surface every 1–2 h during the cruise, using the R/V flowing sampler. Then, the water was supplied into an SBE

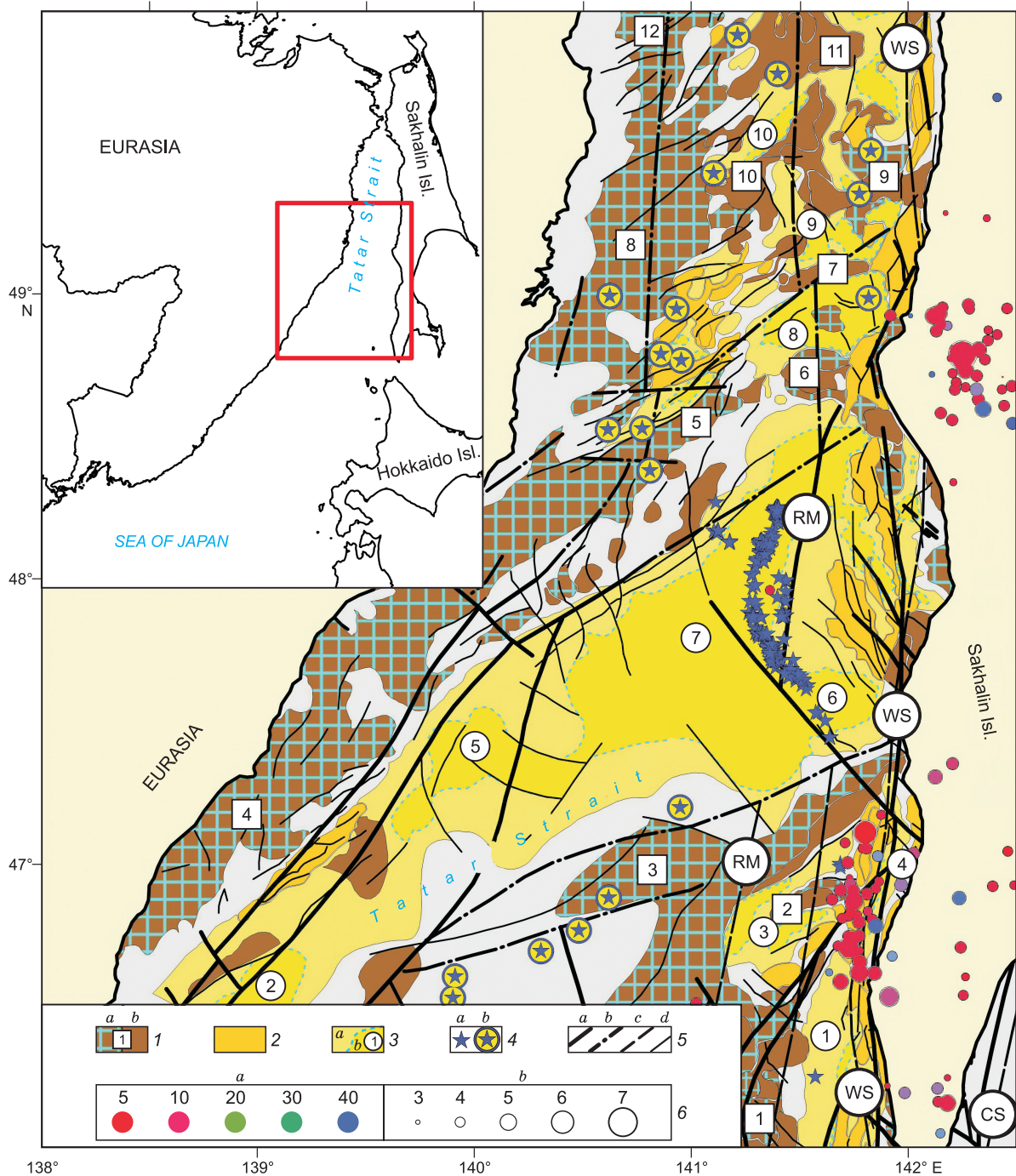


Fig. 1. Schematic structure-tectonic map of the South Tatar sedimentary basin. 1, *a*, tectonic and *b*, volcanotectonic rises: 1, Moneron, 2, Kholmkskysya, 3, Pionerskaya, 4, Primorye, 5, Sovetskaya Gavan', 6, Krasnogorsk, 7, Uglegorsk, 8, Vanino, 9, Chernomorsk, 10, Kamenka, 11, East Syurkum, 12, Syurkum; 2, anticlinal structures in sedimentary cover; 3, *a*, sedimentary basins, *b*, depressions: 1, Moneron, 2, Samarga, 3, Kholmkskyskaya, 4, Yasnomorsk, 5, Nel'ma, 6, Slepikovskii, 7, Ternei trough, 8, Lamanon trough, 9, Lesogorsk, 10, Tumnin; 4, gas shows: *a*, bottom gas seeps, from geochemical data of the Pacific Oceanological Institute, Vladivostok, *b*, "gas" columns (chimneys) in sedimentary cover (Kharakhin, 2010); 5, faults: *a*, proved, *b*, concealed, *c*, predicted, *d*, other: CS, Central Sakhalin, WS, West Sakhalin, RM, Rebut-Moneron (Shaposhnikov et al., 1994, 1995; Zharov et al., 2004; Dymovich et al., 2016); 6, earthquakes: *a*, hypocenter depth, km, *b*, magnitude. Inset shows the position of the study area.

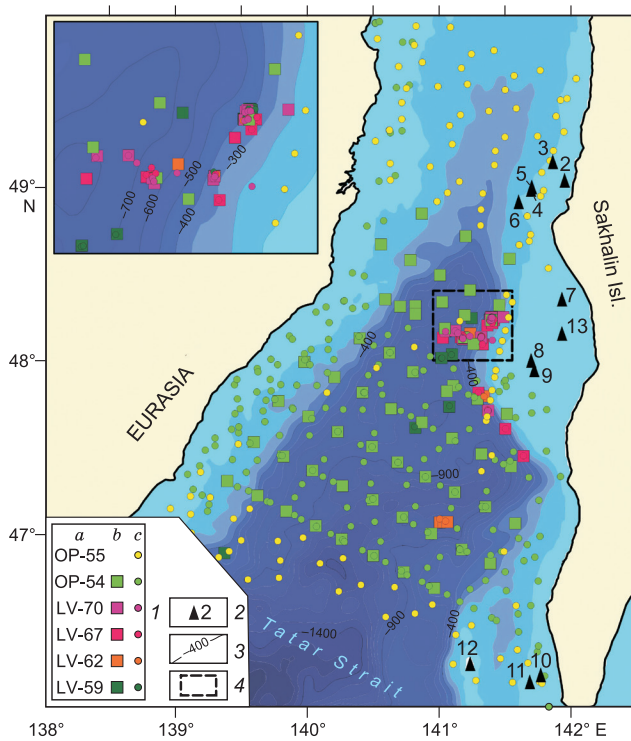


Fig. 2. Scheme of the study area. 1, a, numbers, b, stations of water sampling and stations of bottom sediment sampling; 2, structural and petroleum exploration wells: 2, Gavrilovskaya-1, 3, Gavrilovskaya-2, 4, Izyl'met'evskaya-1, 5, Izyl'met'evskaya-2, 6, Nadezhdinskaya-1, 7, Krasnogorskaya-1, 8, Staromayachinskaya-1, 9, Staromayachinskaya-2, 10, Vinskaya-1, 11, Kuznetsovskaya-1, 12, Moneronskaya, 13, Il'inskaya; 3, isobaths (m); 4, area fragment shown in detail in the inset.

21SEACAT thermosolinograph (Washington, USA) for the continuous determination of temperature and salinity.

At the stations, seawater was sampled with a Rosette sampling system with twelve 10 L Niskin polyvinyl chloride bathometers. The Rosette system was combined with a CTD multiparameter probe.

Water was sampled into 68 ml glass bottles, which were hermetically closed. Then, 12 ml special-purity helium was introduced into the bottles. For analysis for He and H₂, 12 ml air was used as a gas phase. The bottles with samples were shaken on an LS-110 mixing device to reach equilibrium between the liquid and the gas phases. After mixing, an aliquot of the gas phase was taken by a syringe for a chromatographic analysis.

Sediment sampling and analysis technique. Sampling and analysis of bottom sediments were performed by the marine gas-geochemical technique elaborated by the Gas Geochemistry Laboratory of the V.I. Il'ichev Pacific Oceanological Institute, Vladivostok (Jin et al., 2013; Shoji et al., 2014). The bottom sediments were sampled with 550 or 350 cm long hydrostatic and gravity samplers from standard reference horizons (at depths of 10, 25, 50, 100, 150, 200, 250, and 300 cm). Additional samples were taken from the sections with a contrasting change in sediment lithotype and

with the appearance of organic-material interbeds, hydrotronilite members, etc.

The sediment was sampled with 12 ml cut-tip syringes into 43 ml flasks filled with a saturated NaCl solution preserved with 0.5 ml chlorhexidine bigluconate 0.05%. Helium (12 ml), used as a gas phase, was introduced into the flasks using a Tedlar Bag Dual Valve (USA) gas bag. Analysis for He and H₂ was performed in 68–100 ml flasks filled with a saturated NaCl solution; air (12 ml) was used as a gas phase. The flasks with samples were intensively shaken on an LS-110 mixing device (Russia) for at least 4 h and then were treated in a FineSonicE05 ultrasonic bath. Afterwards, the gas phase was sampled with a syringe and introduced into a chromatograph.

Chromatographic analysis for gas hydrocarbons was carried out on board the vessel, using a Crystallux 4000M chromatograph equipped with a flame ionization detector and two thermal-conductivity detectors. Chromatographic analysis for helium and hydrogen was performed on a Chromatec 2000 gas chromatograph with argon as a carrier gas.

The concentrations of methane, helium, and hydrogen dissolved in seawater were calculated by the equilibrium paraphase analysis technique elaborated by Yamamoto et al. (1976) and modified by Wiessenburg and Guinasso (1979), using the solubility constants of the gases. The concentrations of methane and helium in the sediment are given in ppm (1·10⁻⁴%).

Technique for calculation of methane fluxes at the water–atmosphere interface. The sea surface methane fluxes were calculated for each sampling point from the determined concentrations of dissolved methane in the seawater surface layer with regard to temperature, salinity, and methane concentrations in the water–atmosphere interface layer and to the wind speeds at the sampling moment. Continuous meteorological measurements were carried out at the Davis Vantage Pro2 (USA) portable weather station during all cruises. The calculation was made by the technique described by Mishukova et al. (2007) and Vereshchagina et al. (2013), using the formula $F = \Delta C \cdot K^{\text{tot}}$, where $\Delta C = C_{\text{meas}} - C_{\text{eq}}$ is the difference between the measured methane concentration in seawater and the equilibrium concentration of atmospheric methane in seawater at given temperature, salinity, and atmospheric pressure; $K^{\text{tot}} = K_{\text{th}} + K_{\text{br}} + K_{\text{b}}$, where K^{tot} is the total gas exchange coefficient at the water–air interface, K_{th} is the thermal gas exchange coefficient, K_{br} is the gas exchange coefficient for wave breaking, and K_{b} is the gas exchange coefficient for bubble collapse. The oversaturation index N (%) was calculated for each sample by the formula $N = (\Delta C / C_{\text{eq}}) \cdot 100$. The Gas Chemistry Laboratory of the Pacific Oceanological Institute, Vladivostok, has Rosstandart (Federal Agency on Technical Regulating and Metrology) Certificate No. 41 (passport PS 1.047-18).

Data on the epicenters, time, and magnitude of the earthquakes of 2011–2017 were borrowed from http://neic.usgs.gov/neis/bulletin/neic_edau_1.htm to take account of the influence of the local seismic situation in the period of the experimental studies.

RESULTS AND DISCUSSION

Methane at the sea surface and in water column. Over the observation period (2012–2018), methane fluxes at the water–atmosphere interface in the entire water area under study varied from -1.6 to 482 mol/(km²×day); methane concentrations, from 2.3 to 115 nmol/L; and the methane oversaturation index of water (N), from -12 to 4170% . During the cruise OP-55 of R/V Akademik Oparin in 2018, methane undersaturation of water and, as a result, absorption of atmospheric methane were observed at two stations in the northern Tatar Strait. In the rest water area under study, methane concentrations exceeded the equilibrium values C_{eq} . The difference between the measured and equilibrium methane concentrations (ΔC) varied from -0.3 to 112 nmol/L (the minimum was established during the cruise OP-55, and the maximum, during the cruise LV-70), and C_{eq} was within 2.4 – 3.4 nmol/L. Figure 3 shows the distribution of methane concentrations in the seawater surface layer in the southern Tatar Strait in the autumn of 2017.

The maximum methane concentrations in seawater, up to 27 nmol/L, are recorded in the east of the study area. In the northeast and north of the water area, the methane concentrations are lower, although there are local zones with high C_{meas} values, up to 10 nmol/L. In the west of the area, controlled by the submarine extension of the Sikhote-Alin volcanogenic belt, the methane concentrations are still lower. Its equilibrium concentrations varied from 2.4 to 3.4 nmol/L mostly because of water temperature variations. In September–October 2017, the measured methane concentrations were 2 – 9 times higher than the equilibrium ones. The index of methane oversaturation of surface waters (N) was 60 –

880% ; the minimum values, $<100\%$, were established in the southern deep-water part of the study area in the autumn of 2017.

Figure 3 also shows the distribution of surface currents in the period of seawater sampling (late September–mid October). The south-to-north current along the central part of the Tatar Strait is locally branched to the west and to the east, forming numerous multidirectional vortex-type circulations, which is consistent with the earlier reported data (Pishchal'nik et al., 2011).

As shown by Mishukova et al. (2015), strong methane emission in the form of steady gas bubble jets from submarine sources on the western shelf and on the Sakhalin slope leads to the formation of horizontal water layers with high methane concentrations. Figure 4 demonstrates the vertical distribution of methane concentrations in seawater in two areas of the zone of the influence of deep-water flares (Fig. 4a) and flares localized at depths of 300 – 400 m (Fig. 4b), according to the data obtained during the cruises LV-67 and LV-70 of the R/V Akademik M.A. Lavrentiev. Figure 4c schematically shows the location of the observation stations near which gas hydrates were discovered.

As seen from Fig. 4, dissolved methane is unevenly distributed throughout the water column, with its extreme concentrations detected in several water horizons: in the bottom horizon, at a certain distance from the bottom, in intermediate layers, and in the surface layer. The presence of a well-heated desalinated water surface layer in August suppresses the turbulent exchange at the water–atmosphere interface and prevents methane emission into the atmosphere. Methane accumulates in different horizons of the water column. In autumn, methane concentrated in intermediate horizons is

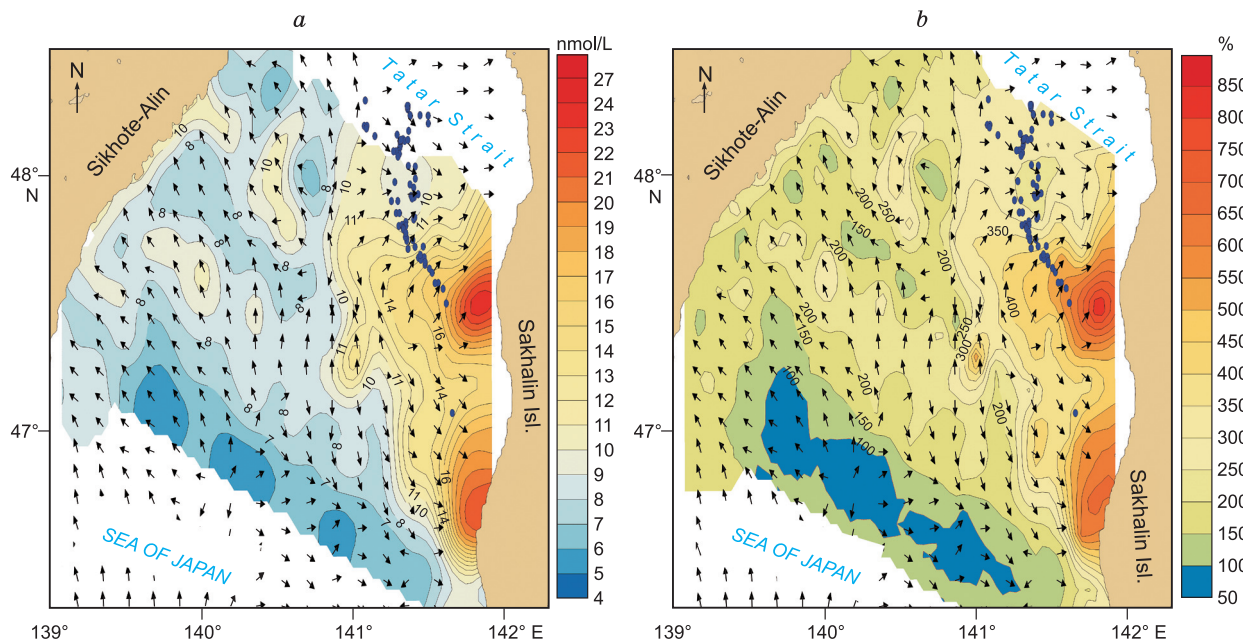


Fig. 3. Distribution of methane (a) and methane oversaturation index (b) in the 4 m thick water surface layer. Arrows show surface currents in the Tatar Strait water area, and circles mark the location of gas flares.

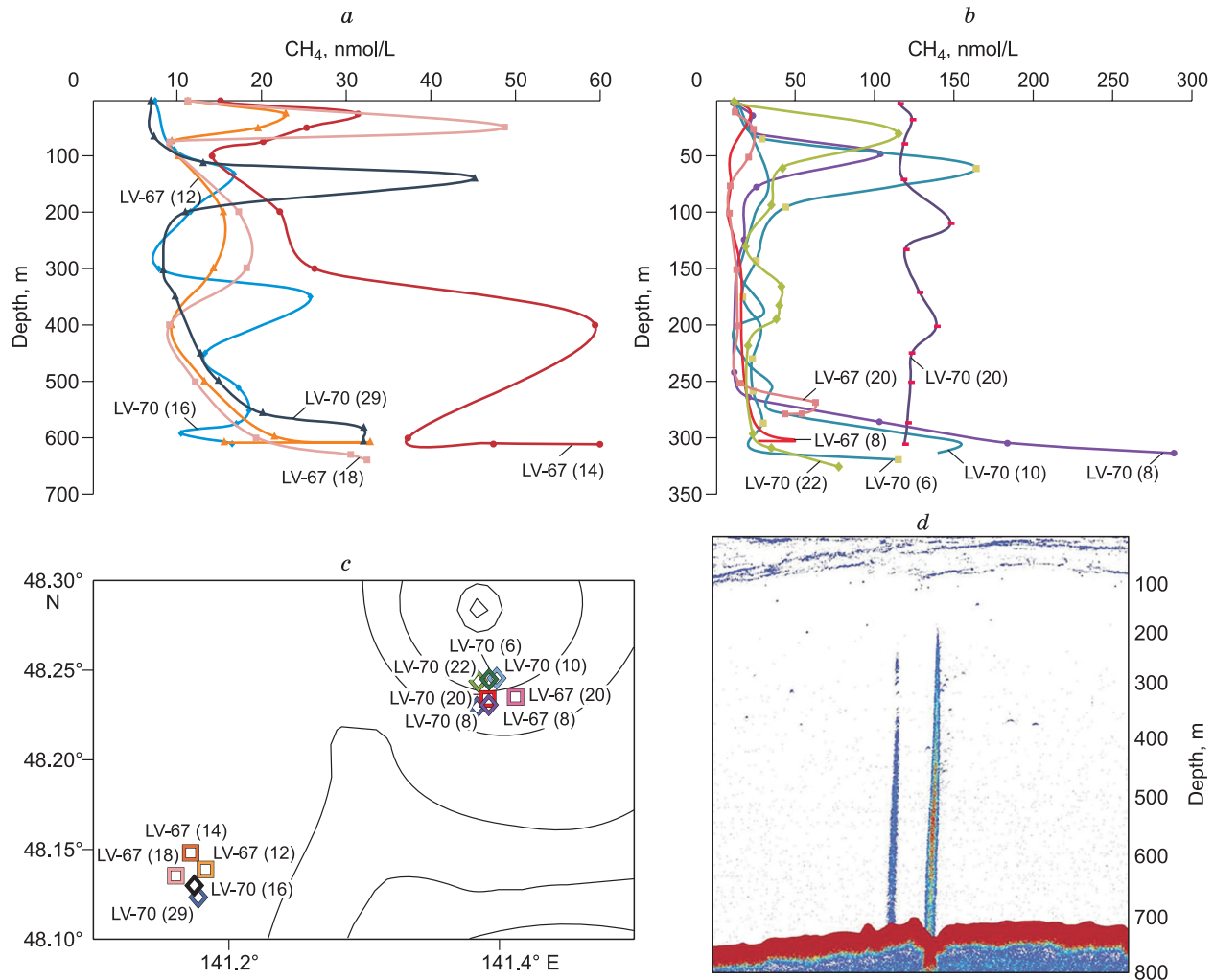


Fig. 4. Vertical distribution of methane in the Tatar Strait water column: *a*, at deep-water (down to 700 m) stations; *b*, at mid-depth (≤ 400 m) stations; *c*, schematic location of these stations during the cruises of R/V Akademik M.A. Lavrentiev (LV-67, June 2014 and LV-70, June 2015), *d*, echograms of a deep-water gas flare in the Tatar Strait (LV-70). *a*–*c*, Parenthesized is the station number.

transferred to the water surface through convection and is released into the atmosphere, which is confirmed by the above data.

Distribution of methane fluxes at the water–atmosphere interface. The results obtained indicate that the southern Tatar Strait is a region of steady atmospheric methane emission. Figure 5 shows the distribution of methane fluxes in this region, based on the methane emission values estimated during the cruise OP-54 in 2017.

The distribution of methane fluxes in the study area is uneven, as in the adjacent areas of the Sea of Japan and in the water area of the Sea of Okhotsk (Mishukova and Vereshchagina, 2011; Obzhirov et al., 2016; Mishukova et al., 2017; Mishukova and Shakirov, 2017). Figure 5 clearly shows that zones with high methane fluxes frame the South Tatar sedimentary basin in the west, north, and east.

Zone (methane discharge site) I was revealed in the central part of the strait, where the methane flux is 25–71 mol/

(km²×day). The maximum methane flux is observed in sub-zone Ia with sea depths of 300–700 m. According to the data of four cruises of the R/V Akademik M.A. Lavrentiev (2012–2015), there are three groups of high methane fluxes in this subzone, which are confined to gas flares where gas hydrates were found. The maximum methane flux is 482 mol/(km²×day).

Zone II is mapped in the east of the study area and occupies the deep-water, slope, and shelf zones. It is characterized by numerous gas flares along the southwestern slope of Sakhalin and by a strong variation in methane fluxes, from 8 to 95 mol/(km²×day).

Zone III is located in the southeast of the study area. Intense methane emission, up to 110 mol/(km²×day), is observed in the shelf water area. In the area of benches resulted from the 2007 earthquake near the town of Nevelsk, the seawater methane concentrations reach 3000 nmol/L (according to our data obtained in 2014), which indicates a gas

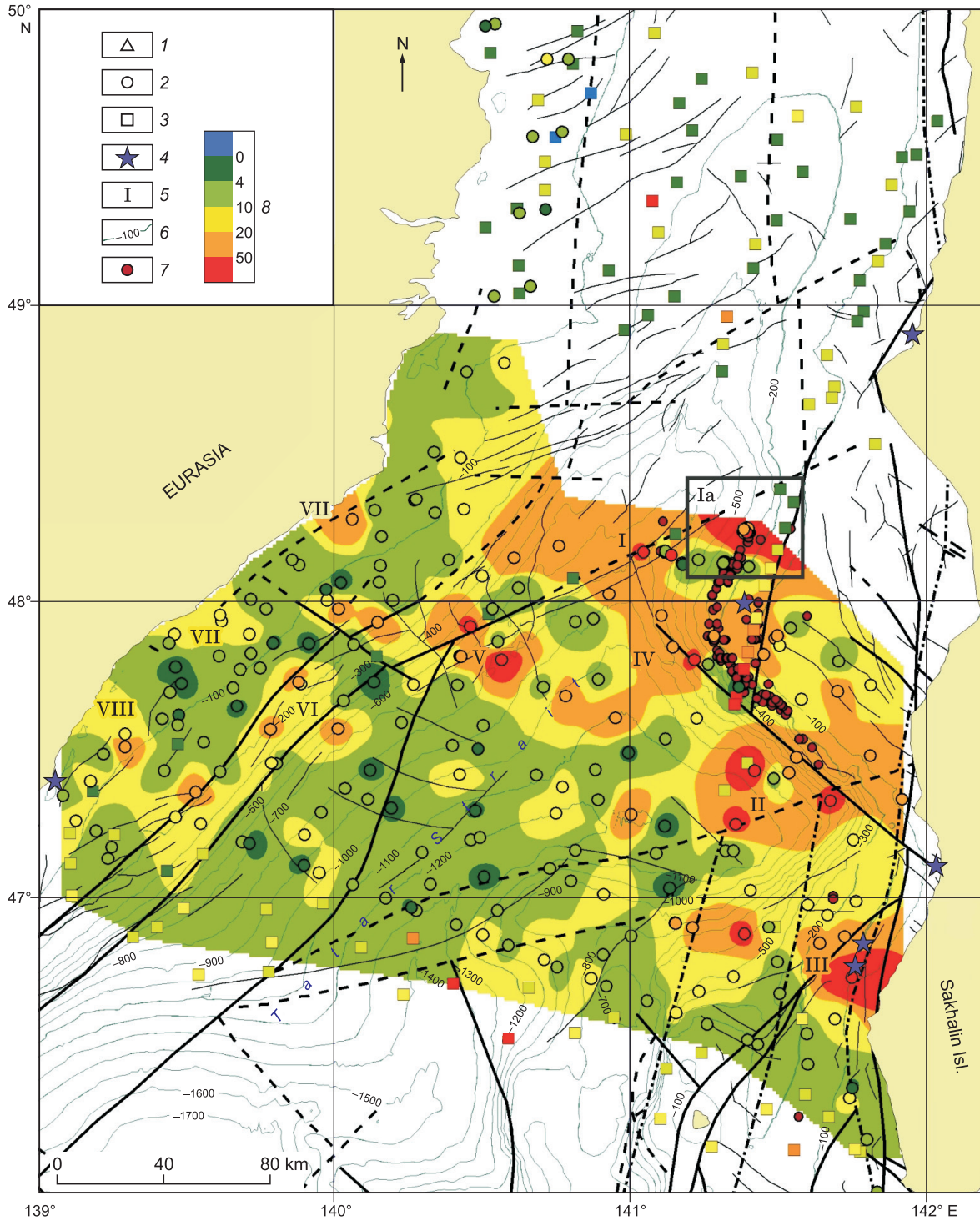


Fig. 5. Map of the bottom relief in the study area, with a methane flux distribution at the water–atmosphere interface ($\text{mol}/(\text{km}^2 \times \text{day})$). Water sampling stations in the cruises: 1, LV-59, LV-62, and LV-67; 2, LV-70 and OP-54; 3, OP-54; 4, epicenters of strong earthquakes of 2011–2017; 5, areas with high methane fluxes (zones I–VIII, see the text for description); 6, isobaths (m); 7, locations of gas flares; δ , methane flux at the water–atmosphere interface ($\text{mol}/(\text{km}^2 \times \text{day})$) (the same gradation for areal distribution (cruise OP-54) and for certain stations). Faults and their types are given in Fig. 1. Rectangle outlines the fragment of the study area where the most detailed survey was made (see inset in Fig. 2 and Fig. 4c).

bubble transfer. In the slope area, methane fluxes from the sea surface are 54 mol/(km²×day). Note that zone III, like zone I, is located in the area of recent strong earthquakes.

Zones IV and V are revealed in the deep-water (>700 m) area south of zone I. The presence of local zones of less intense methane emission (20–40 mol/(km²×day) in the west of the South Tatar sedimentary basin, both in the slope area (zones VI and VII) and in the shelf (zone VIII), suggests the existence of methane sources here. As shown below, this fact is consistent with the distribution of methane-rich zones in the sediments.

In addition to the recognized zones of high methane fluxes into the atmosphere, we mapped local sites of methane emission and runoff. For example, in the autumn of 2018 (cruise OP-55), high methane fluxes, 135 and 106 mol/(km²×day), were recorded at two stations in the south of the study area. In the northern Tatar Strait, two stations recorded high methane fluxes, 54 mol/(km²×day) (OP-54) and 127 mol/(km²×day) (OP-55), and two stations showed absorption of atmospheric methane, –0.3 and –1.6 mol/(km²×day) (OP-55), in the autumn seasons of 2017 and 2018.

In general, methane fluxes in the south of the study area in 2013, 2014, 2015, 2017, and 2018 were higher as compared with 2012. This may be for several reasons: (1) Earthquakes activated gas seepage; (2) the wind speeds in 2012 were higher than those in 2013, 2014, 2015, 2017, and 2018; (3) in summer, methane fluxes from the sea surface are less intense despite the existence of active sources of methane in the water area; and (4) the high methane fluxes in September–October 2017 were due to autumn water convection leading to the removal of methane from intermediate horizons and due to high wind speeds ensuring a rapid renewal of the water surface. The first reason is also indirectly supported by the finding of small inclusions and lenses of gas hydrates in the sediments in 2012 (Jin et al., 2013) and by the discovery of cores rich in large gas hydrate inclusions in the same areas in the following years (Jin et al., 2015).

Methane and helium in bottom sediment cores. In the period 2012–2018, we also studied 119 sediment cores (1420 samples) from the Tatar Strait (Fig. 2), which showed an uneven distribution of gas hydrocarbons and the asymmetric structure of the gas-geochemical field of the South Tatar sedimentary basin. Within the gas chimneys, many sediment cores showed evidence for gas saturation, the contents of free methane were higher than 5 vol.%, the sediments “puffed up” and crackled under pressing because of bursting gas bubbles, and signs and occurrences of authigenic carbonate mineralization (glendonite pseudomorphs) were revealed. Some cores (mostly those located at depths more than 3 m below the bottom surface) were highly gas-saturated and cut by numerous cracks (Jin, 2013). In the northeast of the study area (zone I and subzone Ia), gas hydrate accumulations were found in 11 cores of subsurface sediments (at depths of ≤5 m below the bottom surface).

Methane in contents from 0.35 ppm to 14.9 vol.% (median content of 176 ppm) was found in all bottom sediment

samples. All sampled cores clearly show a regular increase in methane content with sampling depth. Also, positive correlations of methane with ethane and propane were established. The content increase gradient was maximum in cores with gas hydrates and gas-saturated sediment layers. In general, the methane content in the lower sampling horizons was one to five orders of magnitude higher than that in the upper sediment layer.

Figure 6 shows the distribution of methane in the surface layer (0–15 cm) of bottom sediments and the points of measurement of methane fluxes at the water–atmosphere interface in 2012–2018. Methane content in the surface layer varies from 0.35 to 683 ppm (median content of 5.25 ppm). The minimum contents of CH₄ were found in the western deep-water part of the Tatar Strait and did not exceed 4 ppm (Fig. 6). The maximum contents of methane in the surface horizon (0–15 cm) were detected in cores from the area of gas shows and gas hydrate accumulations in the northeastern part of the Ternei depression (zone I). Here, the maximum methane flux at the water–atmosphere interface was also recorded (Fig. 5). A vast area (zone III) of high methane contents (up to 12 ppm) is in the central part of the Tatar Strait, in the central part of the Ternei depression. Other methane anomalies (zones II and IV–VII) in the surface layer of bottom sediments are locally distributed in the northwestern, western, southwestern, and southern parts of the sedimentary basin. These anomalies are usually confined to submarine rise zones and various dislocations.

The high contents of methane and helium in the same areas may be indicators of deep-seated permeability zones and hydrocarbon fluids. Studies in the areas of methane seeps and gas-saturated structures (2012–2017) revealed variable contents of helium in the subsurface sediment layer. The uneven distribution of helium, with its average contents from 5 to 15 ppm in the sediment cores, may indicate fluctuations in the dynamics of the ascending gas flux (Fig. 7).

The high content of He (up to 54 ppm) in the bottom sediment sample from the station OP-54-26HC calls for additional study. Close contents of He were earlier detected in the gas hydrate-bearing sediment section on the northwestern flank of the Kuril basin (Shakirov et al., 2016). High contents of He (independently of the time of observation) were also found by us in the Pugachevsky and Yuzhno-Sakhalinsky mud volcanoes (up to 52 ppm in free gas), in the Sinegorsk springs (up to 105 ppm in water), and in gases of Sakhalin coal deposits (up to 15 ppm in gas emissions) in the vicinity of the study area. For comparison, the atmospheric background content of helium is 5 ppm (Yanitskii, 1979). Sakhalin mud volcanoes are characterized by $^3\text{He}/^4\text{He} = (1.0\text{--}3.8) \cdot 10^{-6}$ (Lavrushin et al., 1996), which is close to the mantle values $^3\text{He}/^4\text{He} = n \cdot 10^{-5}\%$ (Mamyrin and Tolstikhin, 1981). Similar data were obtained for Kamchatka: $^3\text{He}/^4\text{He} \sim 10^{-5}\%$ (Chudaev, 2003).

Geologic control of methane fluxes. The variations in sea surface methane fluxes are probably due to the difference between their lithospheric sources in area and intensity.

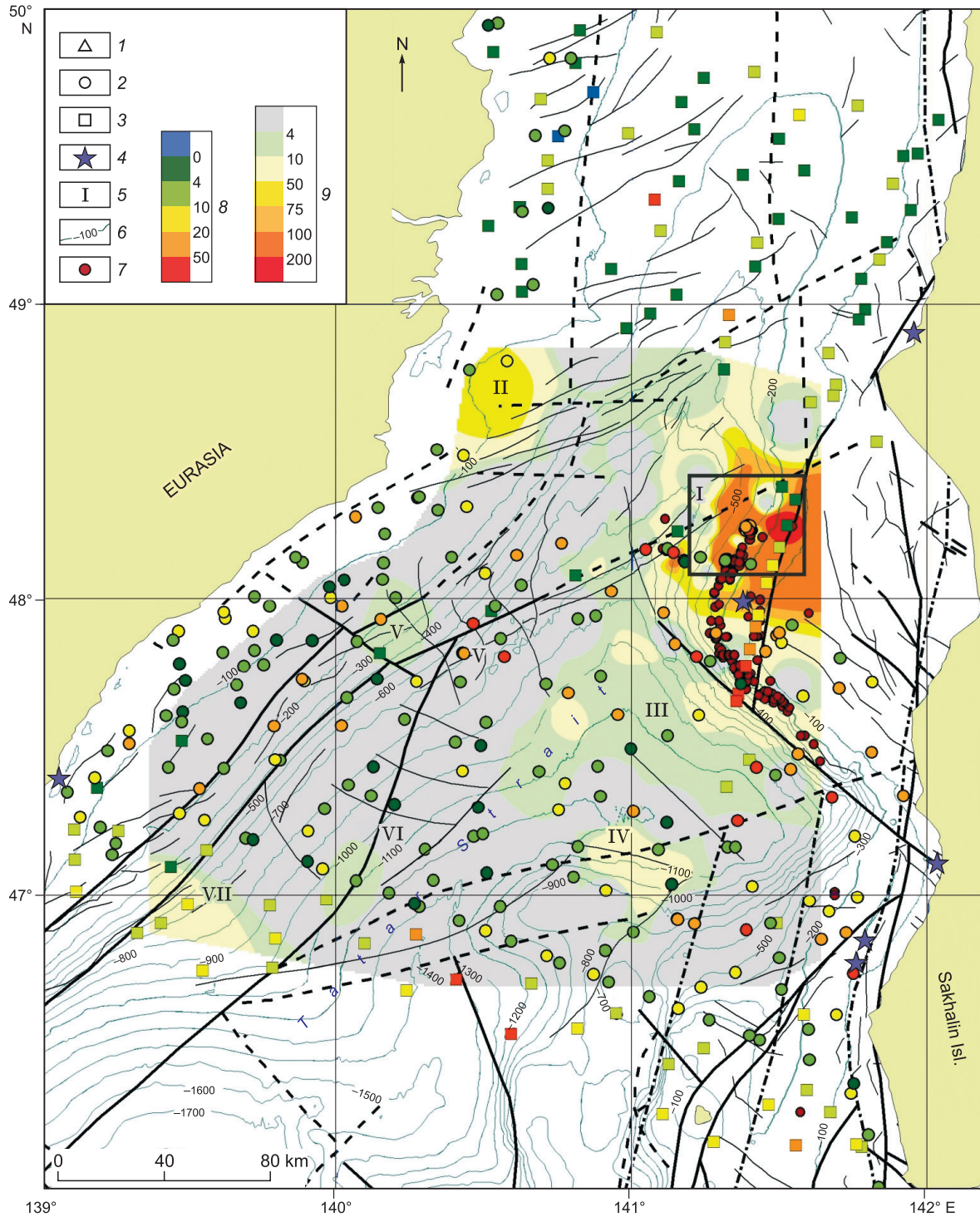


Fig. 6. Distribution of methane fluxes at the water–atmosphere interface ($\text{mol}/(\text{km}^2 \times \text{day})$) and methane contents in the surface layer (0–15 cm) of bottom sediments in the study area. Water sampling stations during the cruises: 1, LV-59, LV-62, and LV-67, 2, LV-70 and OP-54, 3, OP-55; 4, epicenters of strong earthquakes of 2011–2017; 5, areas with high methane contents in the surface layer of bottom sediments; 6, isobaths (m); 7, locations of gas flares; 8, methane flux at the water–atmosphere interface ($\text{mol}/(\text{km}^2 \times \text{day})$) (the same gradation for all stations); 9, distribution of methane in the surface layer of bottom sediments (CH_4 , ppm). Faults and their types are given in Fig. 1. Square (zone I) corresponds to sub-zone Ia with high methane fluxes at the water–atmosphere interface in Fig. 5.

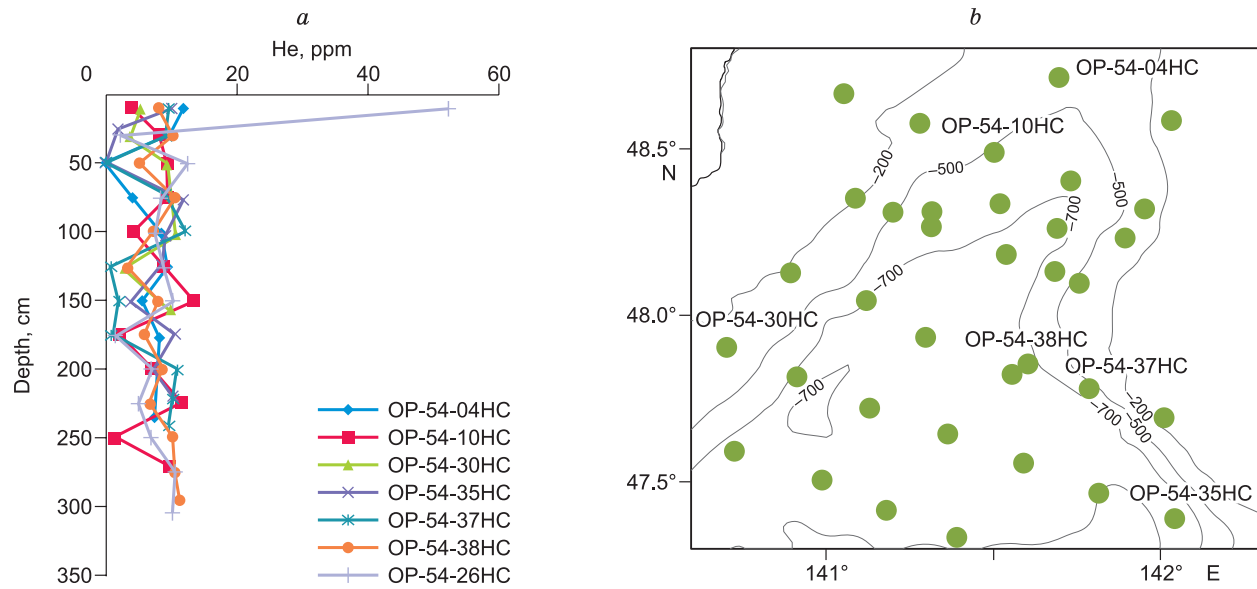


Fig. 7. Distribution of helium in the sediment cores from the South Tatar depression (a) and schematic map of stations (b) (R/V Akademik Oparin, OP-54).

The main gas flare accumulations and the highest methane fluxes from the sea surface were observed in 2013–2017 in the zones where $M = 4.2\text{--}4.7$ earthquakes were recorded at a depth of 9–32 km (zone I and subzone Ia, Fig. 5). These zones of high methane emission spatially coincide with the zone of intense destruction of the suboceanic crust (Fig. 8). The zones in the east of the study area are controlled by blocks of the Hokkaido–Sakhalin fold system with the extending West Sakhalin fault zone in the west (Figs. 1 and 8). Note that subvertical geologic bodies located in the southern and central parts of the study area and marking fluid-dynamic systems (Figs. 2 and 8) lack methane fluxes. This is probably due to the fact that they are located deep in the section and are overlain by sedimentary strata and that the areas of their occurrence are less subjected to strong earthquakes.

Judging by the data obtained and the activity of gas flares, gas migration along faults from sedimentary strata to surface is of pulsed character. The gas sources drained by faults are probably located not lower than the oil window zone, which is confirmed by the carbon isotope composition of methane and ethane and by the high concentrations of hydrogen and helium in seawater and bottom sediments (Shakirov et al., 2016). The variation in methane fluxes at the water–atmosphere interface and in gas flares reflects the variation in the activity of bottom gas sources.

In the west of the study area (the submonoclinical near-flank block in Fig. 8), methane may come from natural-gas accumulations in local geologic structures (Primorskaya, Samarginskaya, etc.) (Kharakhinov, 2010). The sediments sampled at the station LV-59-27HC show no helium and hydrogen anomalies.

Study of most of the cores sampled in the gas flare area of the Tatar Strait (stations 40HC, 29HC, 43HC, 42HC,

31HC, etc.) confirms a predominance of catagenetic gas hydrocarbons: The $\delta^{13}(\text{C}-\text{CH}_4)$ values vary from -43 to -50% VPDB, and $\delta^{13}(\text{C}-\text{C}_2\text{H}_6)$, from -15 to -23% VPDB.

The eastern part of the South Tatar depression, with the most intense atmospheric methane flux, as well as the southwestern part of Sakhalin are parts of the gas-geochemical coal gas zone with a high portion of catagenetic gases (Shakirov and Syrbu, 2012). In the southern and southwestern parts of the island, the average carbon isotope composition of methane in the flux is -21 to -43% VPDB. This composition is due to specific tectonomagmatic and fluid-dynamic activity and the coal gas potential of the southwestern part of the island. Within this area, active vertical discharge of fluids is manifested as hydrocarbon seeps, mud volcanoes, thermal springs, and coal gas shows on the flanks of folded structures and fault zones of different ranks. It was established that the emission of mud volcano fluids and gases increases during seismotectonic activity (Ershov et al., 2011).

Within the study area on the eastern flank of the South Tatar depression, the Staromayachninskaya-1, Staromayachninskaya-2, and Krasnogorskaya wells penetrated coal beds (Kharakhinov, 2010; Nechayuk and Obzhiriov, 2010), which may be the sources of methane in sedimentary basins. The carbon isotope composition of methane from gas hydrate-bearing sediments (e.g., $\delta^{13}(\text{C}-\text{CH}_4) = -47\%$, LV-59-27HC) is similar to that of methane from coal beds in southern Sakhalin ($\delta^{13}(\text{C}-\text{CH}_4) = -35.3$ to -55.9%) (Gresov et al., 2009).

In 2012 and 2013, gas hydrates were sampled within most active gas emission zone Ia (water depth of 320–350 m). The carbon isotope composition of methane and ethane from cores sampled at two stations in this area (R/V Akademik M.A. Lavrentiev, LV-59) points to the catage-

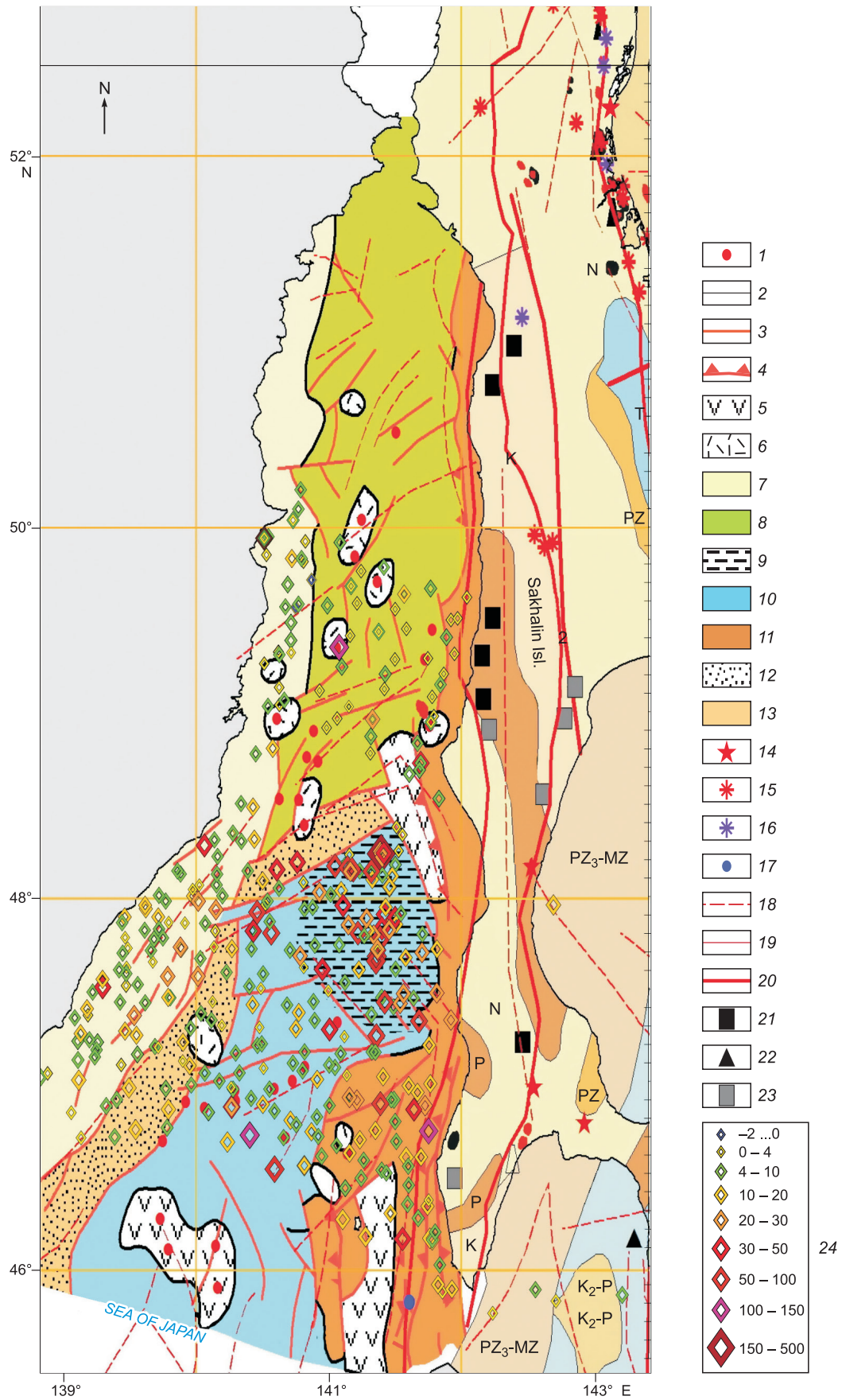


Fig. 8. Distribution of methane fluxes on the map of the geologic structure and fluid-dynamic systems of the Tatar Strait and western Sakhalin, after Kharakhinov (1998, 2010). 1, subvertical geologic bodies, indicators of local fluid-dynamic activity (Kharakhinov, 2010); 2, isopachs of Cenozoic folded area; 3, normal faults; 4, strike-slip faults; 5, Oligocene–Eocene volcanotectonic structures; 6, areas of late Miocene–Pliocene volcanotectonic activity; structural units: 7, submonoclinal western near-flank slope Sikhote-Alin block; 8, North Tatar graben (subbasin), a region of the partial destruction of continental crust; 9, zone of the intense destruction of suboceanic crust; 10, South Tatar deep-water basin (sub-basin) with suboceanic crust; 11, blocks of the Hokkaido–Sakhalin folded system; 12, areas of late Miocene–Pliocene volcanotectonic activity; 13, zoned rift grabens with the partial destruction of continental crust; 14, mud volcanoes; 15, oil shows; 16, gas shows; 17, gas flares; 18, predicted faults, mostly shears; 19, detected faults; 20, fault zones; 21, coal deposits; 22, oil fields; 23, brown-coal deposits; 24, methane fluxes (mol/(km²×day)) during all cruises in 2012–2018.

netic formation of natural gas ($\delta^{13}\text{C}(\text{C}-\text{CH}_4) = -47\%$ VPDB, $\delta^{13}\text{C}(\text{C}-\text{C}_2\text{H}_6) = -23\%$ VPDB). This suggests the supply of catagenetic gases through the water column of the Tatar Strait into the atmosphere.

During the integrated geological and geophysical research, we have first established a correlation of the distribution of gas flares and gas hydrate deposits with the deep structure by the example of the South Tatar sedimentary basin. We have demonstrated that gas shows, gas hydrates, and gas hydrocarbon anomalies in the sediments are confined to the contour of a positive isometric anomaly of the gravity field (Shakirov et al., 2019), which maps the elevated basement block. The gas permeability zone and the conditions favorable for the formation of gas hydrates formed along the arcuate contact zone. This gives grounds to introduce a new predictive geological and geophysical method for search for gas hydrates in seas and oceans, namely, a study of the correlation between the structures of the gravimagnetic and gas-geochemical fields.

CONCLUSIONS

The distribution of high methane, hydrogen, and helium concentrations in bottom sediments and seawater is governed by the spatial distribution and geologic control of submarine gas sources. The geologic and structural position of seeps of catagenetic methane on Sakhalin and the adjacent shelf and slope determines its active emission into the seawater and atmosphere. In general, the flank (western, northern, and eastern) parts of the South Tatar depression show high methane fluxes into the atmosphere.

High sea surface methane fluxes are crucial indicators of the geologic activity. High helium fluxes may indicate mantle fluid migration from petroleum generation zones in the South Tatar depression. The revealed regularities in the distribution of methane, hydrogen, helium, and the thermogenic carbon isotope composition of methane are due to the tectonomagmatic and fluid-dynamic specifics of the Tatar Strait. The distribution density and activity of submarine geologic sources (faults, gas flares, gas hydrates, gas-saturated sediments, etc.) and the specific deep structure of the study area are the main factors responsible for bottom gas-geochemical anomalies.

Sea surface methane fluxes, along with gas-geochemical fields in the sediments and seawater, are indicators of undis-

covered hydrocarbon deposits. The maximum fluxes mark gas hydrate accumulations; they are confined to gas flares and chimneys.

We thank the reviewers for constructive critical remarks, which helped to improve the paper. The expeditions were performed with support from the Earth's Hydrosphere Council of the Federal Agency for Scientific Organizations of the Russian Federation (FASO RF) and with financial support from the FASO RF and, partly, international projects. The study was carried out as part of the basic research "Gas-geochemical fields of the East Asian seas, geodynamic processes, and natural-gas fluxes affecting the formation of geologic structures with hydrocarbon deposits and authigenic mineralization in bottom sediments". It was partly supported by grants 18-05-00153, 18-35-00047 mol_a, 20-35-70014, and 20-55-12010 from the Russian Foundation for Basic Research.

REFERENCES

- Chudaev, V.A., 2003. Migration of Chemical Elements in the Far East Waters [in Russian]. Dal'nauka, Vladivostok.
- Dymovich, V.A., Evseev, S.V., Evseev, V.F., Nesterova, E.N., Margulis, L.S., Atrashenko, A.F., Belyaev, I.V., Derkachev, A.N., Zelepugin, V.N., Konovalenko, A.A., Opalikhina, E.S., Rybak-Franko, Yu.V., Utkin, I.V., Khaibulina, G.A., Zheleboglo, O.V., Yurchenko, Yu.Yu., 2016. State Geological Map of the Russian Federation, Scale 1 : 1,000,000 (Third Generation). Far East Series. Sheet M-54: Aleksandrovsk-Sakhalinsky. Explanatory Note [in Russian]. Kartograficheskaya Fabrika VSEGEI, St. Petersburg.
- Ershov, V.V., Shakirov, R.B., Obzhairov, A.I., 2011. Isotopic-geochemical characteristics of free gases of the South Sakhalin mud volcano and their relationship to regional seismicity. Dokl. Earth Sci. 440 (1), Article 1334.
- Fenwick, L., Capelle, D., Damm, E., Zimmermann, S., Williams, W.J., Vagle, S., Tortell, P.D., 2017. Methane and nitrous oxide distributions across the North American Arctic Ocean during summer, 2015. J. Geophys. Res.: Oceans 122 (1), 390–412.
- Fischer, D., Mogollón, J.M., Strasser, M., Pape, T., Bohrmann, G., Fekete, N., Spiess, V., Kasten, S., 2013. Subduction zone earthquake as potential trigger of submarine hydrocarbon seepage. Nat. Geosci. 6 (8), 647–651.
- Gresov, A.I., Obzhairov, A.I., Shakirov, R.B., 2009. The Methane Resource Base of Coal Basins of the Russian Far East and the Prospects for Its Commercial Development. Vol. I. Carbon Methane Basins of Primorye, Sakhalin, and the Khabarovsk Territory [in Russian]. Dal'nauka, Vladivostok.
- Jin, Y.K., Shoji, H., Obzhairov, A., Baranov, B. (Eds.), 2013. Operation Report of Sakhalin Slope Gas Hydrate Project 2012, R/V Akademik M.A. Lavrentyev Cruise 59. Korea Polar Research Institute, Incheon.

- Jin, Y.K., Minami, H., Baranov, B., Obzhairov, A. (Eds.), 2015. Operation Report of Sakhalin Slope Gas Hydrate Project, 2014, R/V Akademik M.A. Lavrentyev Cruise 67. New Energy Resources Research Center, Kitami Institute of Technology, Kitami.
- Kharakhinov, V.V., 1998. Tectonics of the Okhotsk Sea Petroleum Province. ScD Thesis [in Russian]. Sakhalin NIPImorneft', Okha.
- Kharakhinov, V.V., 2010. Petroleum Geology of the Sakhalin Region [in Russian]. Nauchnyi Mir, Moscow.
- Kvenovolden, K.A., Rogers, B.W., 2005. Gaia's breath — global methane exhalations. *Mar. Petrol. Geol.* 22 (4), 579–590.
- Lavrushin, V.Yu., Polyak, B.G., Prasolov, R.M., Kamenskii, I.L., 1996. Sources of material in mud volcano products (from isotope, hydrochemical, and geological data). *Litologiya i Poleznye Iskopaemye*, No. 6, 625–647.
- Mamyrin, B.A., Tolstikhin, I.N., 1981. Helium Isotopes in Nature [in Russian]. Energoizdat, Moscow.
- Mau, S., Rehder, G., Arroyo, I.G., Gossler, J., Suess, E., 2007a. Indications of a link between seismotectonics and CH₄ release from seeps off Costa Rica. *Geochem. Geophys. Geosyst.* 8, Article Q04003, doi:04010.01029/02006GC001326.
- Mau, S., Valentine, D.L., Clark, J.F., Reed, J., Camilli, R., Washburn, L., 2007b. Dissolved methane distributions and air-sea flux in the plume of a massive seep field, Coal Oil Point, California. *Geophys. Res. Lett.* 34 (22), L22603.
- Mau, S., Heintz, M.B., Valentine, D.L., 2012. Quantification of CH₄ loss and transport in dissolved plumes of the Santa Barbara Channel, California. *Cont. Shelf Res.* 32, 110–120.
- Mau, S., Römer, M., Torres, M.E., Bussmann, I., Pape, T., Damm, E., Geprägs, P., Wintersteller, P., Hsu, C.-W., Loher, M., Bohrmann, G., 2017. Widespread methane seepage along the continental margin off Svalbard – from Bjørnøya to Kongsfjorden. *Sci. Rep.* 7 (42997), 1–13.
- Mel'nikov, O.A., Il'ev, A.Ya., 1989. New manifestations of mud volcanism on Sakhalin. *Tikhookeanskaya Geologiya*, No. 3, 42–48.
- Minami, H., Jin, Y.K., Baranov, B., Nikolaeva, N.A., Obzhairov, A. (Eds.), 2016. Operation Report of Sakhalin Slope Gas Hydrate Project, 2015, R/V Akademik M.A. Lavrentyev Cruise 70. New Energy Resources Research Center, Kitami Institute of Technology, Kitami.
- Mishukova, G.I., Vereshchagina, O.F., 2011. Methane distribution and its fluxes on water–atmosphere interface in areas of a shelf and a slope of the the Sakhalin and the Deryugin basin (the Sea of Okhotsk). *Vestnik DVO RAN*, No. 6, 64–71.
- Mishukova, G.I., Shakirov, R.B., 2017. Spatial variations of methane distribution in marine environment and its fluxes at the water–atmosphere interface in the western Sea of Okhotsk. *Water Resour.* 44 (4), 662–672.
- Mishukova, G.I., Obzhairov, A.I., Mishukov, V.F., 2007. Methane in Fresh and Sea Waters and Its Fluxes at the Water–Atmosphere Interface in the Far East Region [in Russian]. *Dal'nauka*, Vladivostok.
- Mishukova, G.I., Mishukov, V.F., Obzhairov, A.I., 2010. Distribution of methane contents in sea waters and its fluxes on border of water–atmosphere at some regions of the Sea of Okhotsk. *Vestnik DVO RAN*, No. 6, 36–43.
- Mishukova, G.I., Mishukov, V.F., Obzhairov, A.I., Pestrikova, N.L., Vereshchagina, O.F., 2015. Peculiarities of the distribution of methane concentration and methane fluxes at the water–air interface in the Tatar Strait of the Sea of Japan. *Russ. Meteorol. Hydrol.* 40 (6), 427–433.
- Mishukova, G.I., Shakirov, R.B., Obzhairov, A.I., 2017. Methane fluxes on the water–atmosphere boundary in the Sea of Okhotsk. *Dokl. Earth Sci.* 475 (2), 963–967.
- Obzhairov, A.I., 1993. Gas-Geochemical Fields of Sea and Ocean Bottom Water [in Russian]. Nauka, Moscow.
- Obzhairov, A.I., Pestrikova, N.L., Mishukova, G.I., Mishukov, V.F., Okulov, A.K., 2016. Distribution of methane content and methane fluxes in the Sea of Japan, Sea of Okhotsk, and near-Kuril Pacific. *Russ. Meteorol. Hydrol.* 41 (3), 205–212.
- Pishchal'nik, V.M., Leonov, A.V., Arkhipkin, V.S., Melkii, A.V., 2011. Mathematical Modeling of the Ecosystem Conditions in the Tatar Strait [in Russian]. *Izd. SakhGU, Yuzhno-Sakhalinsk*.
- Rodnikov, A.G., Zabarinskaya, L.P., Sergeeva, N.A., 2014. The deep structure of the Earth's earthquake regions (Sakhalin Island). *Vestnik ONZ RAN* 6, Article NZ1001.
- Shakirov, R.B., Syrbu, N.S., 2012. Natural sources of methane and carbon dioxide on Sakhalin Island and their role in the formation of ecologic gas-geochemical zones. *Geoekologiya. Inzhenernaya Geologiya. Hidrogeologiya. Geokriologiya*, No. 4, 344–353.
- Shakirov, R.B., Syrbu, N.S., Obzhairov, A.I., 2016. Distribution of helium and hydrogen in sediments and water on the Sakhalin slope. *Lithol. Mineral Resour.* 52 (1), 61–73.
- Shakirov, R.B., Valitov, M.G., Obzhairov, A.I., Mishukov, V.F., Yatsuk, A.V., Syrbu, N.S., Mishukova, O.V., 2019. Methane anomalies, its flux on the sea–atmosphere interface and their relations to the geological structure of the South-Tatar sedimentary basin (Tatar Strait, the Sea of Japan). *Mar. Geophys. Res.* 40 (4), 581–600.
- Shaposhnikov, G.N., Aleksandrov, G.P., Egorov, S.V., Il'in, K.B., Solov'ev, V.V., Strel'nikov, S.I., 1994. State Geological Map, Scale 1 : 1,000,000 (New Series). Sheets L-(53) and L-(54): Kavalerovo. Explanatory Note [in Russian]. Kartograficheskaya Fabrika VSEGEI, St. Petersburg.
- Shaposhnikov, G.N., Aleksandrov, G.P., Egorov, S.V., 1995. State Geological Map of the Russian Federation, Scale 1 : 1,000,000 (New Series). Sheets L-(54), L-(55), and K-(55): Yuzhno-Sakhalinsk. Explanatory Note [in Russian]. Kartograficheskaya Fabrika VSEGEI, St. Petersburg.
- Shoji, H., Jin, Y.K., Baranov, B., Nikolaeva, N.A., Obzhairov, A. (Eds.), 2014. Operation Report of Sakhalin Slope Gas Hydrate Project, 2013, R/V Akademik M.A. Lavrentyev Cruise 62. New Energy Resources Research Center, Kitami Institute of Technology, Kitami.
- Suess, E., Torres, M.E., Bohrmann, G., Collier, R.W., Rickert, D., Goldfinger, C., Linke, P., Heuser, A., Sahling, H., Heeschen, K., Jung, C., Nakamura, K., Greinert, J., Pfannkuche, O., Trehu, A., Klinkhammer, G., Whiticar, M.J., Eisenhauer, A., Teichert, B., Elvert, M., 2001. Sea floor methane hydrates at Hydrate Ridge, Cascadia Margin, in: Pauli, C.K., Dillon, W.P. (Eds.), *Natural Gas Hydrates: Occurrence, Distribution and Detection*. American Geophysical Union, Washington, DC, Geophysical Monograph 124, pp. 87–98.
- Vereshchagina, O.F., Korovitskaya, E.V., Mishukova, G.I., 2013. Methane in water columns and sediments of the north western Sea of Japan. *Deep Sea Res. Part II* 86–87, 25–33.
- Wiessenburg, D.A., Guinasso, N.L., 1979. Equilibrium solubility of methane, carbon dioxide, and hydrogen in water and sea water. *J. Chem. Eng. Data* 24 (4), 356–360.
- Yamamoto, S., Alcauskas, J.B., Crozier, T.E., 1976. Solubility of methane in distilled water and seawater. *J. Chem. Eng. Data* 21 (1), 78–80.
- Yanitskii, I.N., 1979. Helium Survey [in Russian]. Nedra, Moscow.
- Zharov, A.E., Kirillova, G.L., Margulis, L.S., Chuiko, L.S., Kudel'kin, V.V., Varnavskii, V.G., Gagaev, V.N., 2004. Geology, Geodynamics, and Petroleum Potential of Sedimentary Basins of the Tatar Strait [in Russian]. DVO RAN, Vladivostok.